Annals of the University of Craiova, Mathematics and Computer Science Series
Volume 46(1), 2019, Pages 41–55
ISSN: 1223-6934

Mathematical modelling of nitrogen removal in horizontal subsurface flow constructed wetland

Ihsane Mouaouia, W. Olivier Sawadogo, Abderrahim Charkaoui, and Nour Eddine Alaa

Abstract. The research work presented herein makes a contribution to HSSF CW greywater treatment by developing a conceptual and numerical model to simulate the spatial and temporal variations of nitrogen concentration. This paper presents the simulation of flow and nitrogen removal processes by using the advection-dispersion- reaction modeling approach. The flow equation is solved by using the mixed finite ele- ment method. The system of advection-dispersion-reaction is solved by using the technique of separation of the operators. The equation of advection is approximed by the Characteristics-Galerkin Method. The dispersion-reaction equation was carried by using the finite element method. The softwares freefem++ and matlab were used. This phenomenon was materialized by a horizontal subsurface Flow Constructed Wetland treating greywater in a Moroccan primary school. The decay coefficient are been identified by solving an inverse problem using observed data. The Particle Swarm Optimization and Gravitational Search Algorithm (PSOGSA) proposed by Mirjalili et al. [24] is used to solve the inverse problem. Numerical simulation was validated after calibration on the basis of obtained experimental data by controlling water quality parameters over a period of 100 days. Comparative analysis shows that the total predicted effluent of nitrogen concentration obtained by the numerical simulation agrees fully with the one obtained by experimental data.

2010 Mathematics Subject Classification. 62P12, 35A15, 65M06, 65M60.
Key words and phrases. Horizontal sub-surface flow constructed wetland, nitrogen removal, mathematical modeling, advection-dispersion-reaction system, inverse problem PSOGSA algorithm.

1. Introduction

The processes that govern the transformation of nitrogen compounds in artificial marshes are multiple and refer to the nitrogen cycle in porous media. For the sake of synthesis, the complex processes related to the fixation of atmospheric nitrogen by plants and free bacteria of the filter substrate will not be developed. Only the phenomena of degradation of the nitrogen compounds contained in the wastewater will be exposed.

Nitrogen supplied to artificial wetlands by wastewater is usually in organic form. It undergoes ammonification, then nitrification and finally denitrification according to the biochemical conditions of the environment ([30], [5], [20]).

This paper has been presented at the Conference MOCASIM, Marrakesh, 26-27 November 2018.

Ammonization consists of the mineralization of organic nitrogen into ammonia (NH3) under the action of a living heterotrophic bacterial flora in the filtration substrate. It occurs in both aerobic and anaerobic environments. In turn, the ammonia undergoes various transformations to give ammonium (NH4 +).

In recent years, constructed wetland (CW) has become a major way of groundwater treatment. In [23], Mouaouia et al. studied mathematical modeling and numerical simulation of the evolution of phosphorus concentration in a Wetland treating Greywater Constructed at a primary school of Marrakesh.

The aim of this work is to increase the understanding of the nitrogen removal in the same system.

The model focuses on water flow and reactive solute transport. Nitrogen is present in wastewater as ammonium, NO_2^- and NO_3^-. The mathematical model that governs the evolution of the concentrations is a system of hierarchical equations of convection-dispersion-reaction. This system of equations is coupled with the hydraulic head equation.

The structure of our paper is outlined as follows. In Section 2 the mathematical modeling is introduced, Existence and uniqueness of the solution of hierarchical equations of convection-dispersion-reaction used is presented. In Section 3 is devoted to the numerical resolution of the equations. The section 4 present the inverse problem. Existence and uniqueness of this problem have been established. In Section 5 we present Particle Swarm Optimization and Gravitational Search Algorithm (PSOGSA) used to solve inverse problem. The results and discussion of numerical experiments are presented in Section 6.

2. Mathematical modeling

2.1. Experimental data. To meet the objectives of this research, a HSSF CW was built at a Primary school in Marrakesh (Morocco) (31^o42024 "N, 7^o58050 "W, 451m), with an average annual temperature of 19.6^oC and annual precipitation of 282 mm. At the upstream of the HSSF, all the school grey water was collected from hand wash sinks and directed to a pre-treatment unit.

In order to evaluate the performance of simulation approaches and mathematical models, experimental data were taken. We took measures at the inlet and the outlet every five days.

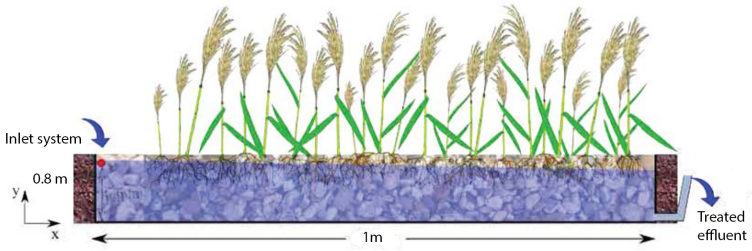

FIGURE 1. Site.

2.2. Mathematical modeling of flow. In order to obtain the experimental data for this study, we used a HSF CW similar to those find in the paper of Akratos and Tsihrintzis [1]. Our facility is a rectangular tank (with dimensions 5 m long, 0.75 m wide and 0.6 m deep). Three different porous media layers were used, namely medium gravel (MG),fine gravel (FG) and cobbles (CO). Each one represents a full compartement of 0.2m tickness and 5m long. The tank is planted using the cattails (C, Typha latifolia). Regarding other data for the CW layers, we have the following values respectively for MG, FG and CO: porosity(ω) 0.39, 0.33 and 0.29, permeability(K) : $10^{-7}m^2$,6.25 $10^{-7}m^2$, and 2.25 $10^{-5}m^2$.

2.2.1. *Condition of flow.* Wastewater enters the domain through boundary 3 (a length of 0.2 m in the x^{th} direction representing the mixing zone) where a constant hydraulic head of 0.6 m is defined and the effluent leaves through boundary 5 (a length of 0.1 m in the y^{th} direction), where a constant hydraulic head of 0.4 m is defined. Boundaries 1, 2,4 and 6 represent a null flux.

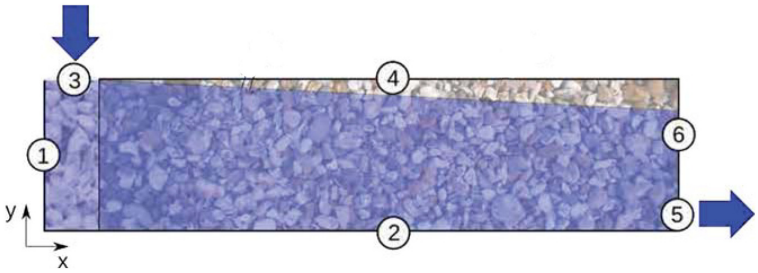

FIGURE 2. Conditions of flow.

2.2.2. *Mathematical model.* Under the above mentioned flow conditions and applying the mass conservation law and the Darcy's law ([18, 21]), the flow in transitory mode in the domain is governed by the following system of equations:

$$\begin{cases} S(x,y)\frac{\partial h(x,y,t)}{\partial t} - div(K(x,y).\nabla h(x,y,t)) = f(x,y,t) & \text{in} \quad \Omega\times]0,T[\\ h(x,y,0) = h_0(x,y) & \text{in} \quad \Omega \\ h(x,y,t) = h_D(x,y,t) & \text{on} \quad \Gamma^D\times]0,T[\\ -K(x,y)\frac{\partial h(x,y,t)}{\partial n} = h_N(x,y,t) & \text{on} \quad \Gamma^N\times]0,T[\end{cases} \tag{1}$$

where

- T is the date of measure.
- Ω, representing the domain
- h is the hydraulic potential
- f is the source term
- h_0 the initial condition corresponding to the date $t = 0$
- h_D is the Dirichlet boundary condition, representing the imposed potential
- Γ^N represent boundaries 1,2,4 and 6
- Γ^D = represent boundaries 3 and 5

- K and S represent respectively the permeability function and the coefficient of storage.

Once the equation (1) is resolved, let h denote this solution, we deduce respectively the Darcy's velocity u and the velocity by the following relations:

$$\begin{array}{rll} u(x,y,t) = -K(x,y).\nabla h(x,y,t) & \text{in} & \Omega \times [0,T] \\ v(x,y,t) = \frac{u(x,y,t)}{\omega} & \text{in} & \Omega \times [0,T] \end{array} \tag{2}$$

where ω is the effective porosity.

2.3. Transport modeling.

2.3.1. *Mathematical model.* The evolution of the contaminant concentrationt is governed by the reaction-adsorption-diffusion following equation ([18, 21]):

$$\begin{cases} \frac{\partial C}{\partial t} = \nabla.(D.\nabla C) - \nabla.(vC) - \lambda C & \text{in} \quad \Omega\times]0,T[\\ C(x,y,0) = C_0(x,y) & \text{in} \quad \Omega \\ -D\frac{\partial C}{\partial n} + (v.n)C = 0 & \text{on} \quad \Gamma^0\times]0,T[\end{cases} \tag{3}$$

where:

- C the concentration (ML^{-3}),
- C_0 the initial concentration (ML^{-3}),
- D the dispersion tensor (L^2T^{-1}),

$$D = \begin{pmatrix} D_{xx} & D_{xy} \\ D_{yx} & D_{yy} \end{pmatrix}$$

- λ, the decay coefficient constant (T^{-1})
- v the velocity
- Γ^0 represent boundaries 1,2,3,4,5 and 6.

A general dispersion tensor D is given by

$$D_{xx} = \frac{\alpha_L v_x^2 + \alpha_T v_y^2}{\sqrt{v_x^2 + v_y^2}} + D_m,$$

$$D_{yy} = \frac{\alpha_L v_y^2 + \alpha_T v_x^2}{\sqrt{v_x^2 + v_y^2}} + D_m,$$

$$D_{xy} = D_{yx} = (\alpha_L - \alpha_T)\frac{v_x v_y}{\sqrt{v_x^2 + v_y^2}},$$

where α_L and α_T is the longitudinal and transverse dispersivities (L), D_m is the molecular diffusion (L^2T^{-1}). The last term to the right is the sink-source term R used for the simulation of chemical reactions. He takest's acount plant uptake, substrate adsorption and desorption. This term usually depends on the concentrations of the reagents involved in the chemical reaction, in this case is expressed by the simple relation: $R = -\lambda C$, where λ is a coefficient of decomposition.

Nitrogen is present in wastewater as ammonium, NO_2^- and NO_3^- with concentrations respectively denoted as c_1, c_2 and c_3. We assume that the kinetics of nitrogen simulated by the following reaction chain (nitrification denitrification):

$$NH_4^+ \to NO_2^- \to NO_3^- \to N_2$$

where N_2 represents nitrogen in gaseous form, which is removed from the system. Under these conditions, the concentrations of the substances in the bio-reactor are governed by the following system of equations:

$$\begin{cases} l\frac{\partial c_1}{\partial t} = \nabla.(D.\nabla c_1) - \nabla.(vc_1) - \lambda_1 c_1 & \text{in} \quad \Omega\times]0,T[, \\ \frac{\partial c_2}{\partial t} = \nabla.(D.\nabla c_2) - \nabla.(vc_2) + \lambda_1 c_1 - \lambda_2 c_2 & \text{in} \quad \Omega\times]0,T[, \\ \frac{\partial c_3}{\partial t} = \nabla.(D.\nabla c_3) - \nabla.(vc_3) + \lambda_2 c_2 - \lambda_3 c_3 & \text{in} \quad \Omega\times]0,T[, \\ c_i(x,y,0) = c_i^0(x,y) & \text{in} \quad \Omega, i \in \{1,2,3\}, \\ -D\frac{\partial c_i}{\partial n} + (v.n)c_i = 0 & \text{on} \quad \Gamma^0\times]0,T[, i \in \{1,2,3\}. \end{cases} \tag{4}$$

This mathematical model (4) was originally proposed by Cho (1971). In a particular case, van Genuchten (1985) gave an analytical solution. The application of this model to simulate processes in constructed wetlands was first used by Akratos and Tsihrintzis [1], using experimental data. They validated the performance of these approaches by comparing the results of the simulation with existing experimental data from five pilot-scale CW facilities containing different vegetation and porous material types. The characteristic values of the disintegration coefficients λ_i are estimated, which incorporate the influence of vegetation and temperature and are useful in the design of constructed wetlands or the simulation of nitrogen fate in geological formations.

3. Numerical modeling

3.1. Equation of flow solving. In this part, we propose to solve numerically the equation (1) by using the finite element method for the space discretization. A implicit scheme of Euler will be used for the temporal discretization.

By using a implicit scheme of Euler on the equation (1), we obtain

$$\begin{cases} S\frac{h^{n+1}-h^n}{\Delta t} - div(K\nabla h^{n+1}) = f^{n+1} & \text{in} \quad \Omega \\ h^{n+1} = h_D & \text{on} \quad \Gamma^D \\ -K\frac{\partial h^{n+1}}{\partial \nu} = h_N & \text{on} \quad \Gamma^N \end{cases}, n = 0, \ldots, M-1. \tag{5}$$

Deduce the Darcy's velocity

$$u^{n+1}(x,y) = -K(x,y).\nabla h^{n+1}(x,y),$$

where Δt is the step of time giving by $\Delta t = \frac{T}{M}$, $t_n = n\frac{T}{\Delta t}$ and $f^n = f(x,y,t_n)$, (M a integer strictly positive).
Let's suppose:

$$\mathcal{V} = \left\{\psi \in H^1(\Omega); \psi = 0 \text{ on } \Gamma^D\right\}.$$

Since $mes(\Gamma^D) > 0$, according to [8], we can choose

$$\|\psi\|_V = \left(\int_\Omega |\nabla\psi|^2\right)^{1/2} \text{ as norm on } V.$$

Let $\psi \in \mathcal{V}$ be a test function. Multiplying (5) by v and integrating by parts, the variational formulation associated to the problem (5) is given by

$$\begin{cases} \text{find } h^{n+1} \in H^1(\Omega) \text{ with } h^{n+1} = h_D \text{ on } \Gamma^D \text{ such that } \forall\psi \in V \\ \int_\Omega \beta h^{n+1}\psi + \int_\Omega K\nabla h^{n+1}.\nabla\psi = \int_\Omega \beta h^n\psi + \int_\Omega \beta f^{n+1}\psi + \int_{\Gamma^N} h_N\psi \end{cases} \tag{6}$$

where $\beta = \frac{S}{\Delta t}$. Thus the theorem of Lax-Milgram ensures the existence and uniqueness of a solution to the variational problem (6) and consequently the existence and uniqueness of a solution of (5).

We denote by γ_d the trace operator. Let $r_d \in H^1(\Omega)$ such as $\gamma_d(r_d) = h_D$ and we denote $h_d^{n+1} = h^{n+1} - r_d$.

Let T_h be a triangulation of Ω and we denote P_1 the space of continuous piewise affine function in Ω i.e the space of continuous functions which are affine in x, y on each triangle of T_h. We pose $V_h = P_1 \cap V$. V_h is a linear vector space of finite dimension. We denote N its dimension and $\phi_1, \ldots, \phi_N$ a basis. The approximated problem is:

$$\text{find } \tilde{h}^{n+1} \in V_h, \text{ such that } \tilde{h}^{n+1}(x,y) = \sum_{i=1}^{N} h_i \phi_i(x,y), \tag{7}$$

and take $\tilde{h}^{n+1} = h^{n+1}$ and $v = \phi_i$ for $i = 1, \ldots, N$, we remark that (7) is equivalent to the resolution of the linear system

$$AX = B \tag{8}$$

where $X = (h_i)_{i=1,\ldots,N}$,

$$A_{ij} = \int_\Omega \beta \phi_i \phi_j + \int_\Omega K \nabla \phi_j . \nabla \phi_j = \sum_{T \in T_h} \int_T \beta \phi_i \phi_j + \int_T K \nabla \phi_j . \nabla \phi_j$$

and

$$\begin{aligned} B_i &= \int_\Omega \beta h^n \phi_i + \int_\Omega \beta f^{n+1} \phi_i + \int_\Omega K \nabla r_d . \nabla \phi_i + \int_\Omega \beta r_d \phi_i + \int_{\Gamma^N} h_N \phi_i \\ &= \sum_{T \in T_h} \int_T \beta h^n \phi_i + \int_T \beta f^{n+1} \phi_i + \int_T K \nabla r_d . \nabla \phi_i + \int_T \beta r_d \phi_i + \int_{T \cap \Gamma^N} h_N \phi_i . \end{aligned}$$

3.2. Equation of transport solving. We used operator spliting, [14, 10]. The transport equation (3) is divided into two distinct equations.
At each step of time, we solve firstly by using Characteristics-Galerkin Method the equation of advection.

$$\begin{cases} \frac{\partial C_{i,a}^k}{\partial t} + div(v C_{i,a}^k) = 0 & \text{in} \quad \Omega \times]0,T[, \\ C_{i,a}^k(x,y,0) = C^{k-1} & \text{in} \quad \Omega. \end{cases} \tag{9}$$

We obtain a solution that we note $C_{i,a}^k$.
And secondly, We used implicit finite difference method for the discretization of the time variable and a discretization in finite element P_1 for the space to appriximate dispersion-reaction equation

$$\begin{cases} \frac{\partial C_i^n}{\partial t} - div(D \nabla C_i^n) + \lambda_i C_i^n = f_i & \text{in} \quad \Omega \times]0,T[, \\ C_i^n(x,y,0) = C_{i,a}^k & \text{in} \quad \Omega, \\ -D \frac{\partial C^n}{\partial \eta} + (v C_i^n).n = C_{i,a}^n & \text{on} \quad \Gamma^N \times]0,T[. \end{cases} \tag{10}$$

The parameters λ_i, $i \in \{1,2,3\}$ are been identified by solving an inverse problem using data observed.

4. Idenfication of parameters

In this section, we focus on the identification of parameters, so we formulate our problem to a minimization problem, after we present the derivative in order to make some numerical example. Let's start by the minimisation problem.

4.1. Minimization problem. Throughout this section we are interesting in the following minimization problem

$$\min_{\Lambda\in D\subset\mathbb{R}^3} J(\Lambda), \tag{11}$$

the cost functionnal J is given by a least square criterion

$$J(\Lambda)=\frac{1}{2}\sum_{i=1}^{3}\int_0^T\int_\Omega (c_i-c_i^{obs})^2 d\sigma dt$$

where $C=(c_1,c_2,c_3)$ solution of (4), c_i^{obs} is the data observed and $\Lambda=(\lambda_1,\lambda_2,\lambda_3)$ the vector of parameters.

Theorem 4.1. *Suppose that $0<a\leq\lambda_i\leq b$, $i\in\{1,2,3\}$. The function J defined by*

$$\begin{array}{rccc} J & : & [a,b]^3 & \longrightarrow & \mathbb{R} \\ & & \Lambda=(\lambda_1,\lambda_2,\lambda_3) & \longmapsto & \frac{1}{2}\sum_{i=1}^{3}\int_0^T\int_\Omega (c_i-c_i^{obs})^2 dxdt \end{array}$$

is differentiable with respect to Λ and for all $\xi=(\xi_1,\xi_2,\xi_3)\in[a,b]^3$, we have

$$\nabla J(\Lambda).\xi=\int_{T_{j-1}}^{T_j}\int_\Omega\Big(\xi_1c_1(p_1-p_2)+\xi_2c_2(p_2-p_3)+\xi_3c_3p_3\Big)$$

with (c_1,c_2,c_3) is solution of (4) and (p_1,p_2,p_3) is solution of the following problem

$$\begin{cases} -\frac{\partial p_1}{\partial t}=\nabla.(D.\nabla p_1)-\nabla p_1\nabla v+\lambda_1p_2-\lambda_1p_1+c_1^{obs}-c_1 & in \quad \Omega\times]0,T[, \\ -\frac{\partial p_2}{\partial t}=\nabla.(D.\nabla p_2)-\nabla p_2\nabla v+\lambda_2p_3-\lambda_2p_2+c_2^{obs}-c_2 & in \quad \Omega\times]0,T[, \\ -\frac{\partial p_3}{\partial t}=\nabla.(D.\nabla p_3)-\nabla p_3\nabla v-\lambda_3p_3+c_3^{obs}-c_3 & in \quad \Omega\times]0,T[, \\ p_i(x,y,T)=0 & in \quad \Omega, i\in\{1,2,3\}, \\ D\frac{\partial p_i}{\partial n}=0 & on \quad \Gamma^0\times]0,T[. \end{cases}$$

Proof. We follow the Lagrangian method to prove the differentiability of J, this method gives a rapid derivation of J by introducing a Lagrangian function $\mathcal{L}$ to separate the dependance of the state variables (c_1,c_2,c_3) and $\Lambda=(\lambda_1,\lambda_2,\lambda_3)$. We put by convention $\lambda_0=0$ and we consider

$$\begin{aligned}\mathcal{L}(C,P,\Lambda,\sigma)=&\frac{1}{2}\sum_{i=1}^{3}\int_0^T\int_\Omega(c_i-c_i^{obs})^2d\sigma dt+\sum_{i=1}^{3}\int_0^T\int_\Omega\left(\frac{\partial c_i}{\partial t}p_i+D\nabla c_i\nabla p_i\right)\\&+\sum_{i=1}^{3}\int_0^T\int_\Omega\Big(\nabla v\nabla p_ic_i+(\lambda_ic_i-\lambda_{i-1}c_{i-1})p_i\Big)+\sum_{i=1}^{3}\int_\Omega\sigma_i(c_i(0)-c_i^0).\end{aligned}$$

For all $(C,P,\Lambda,\sigma)\in L^2(0,T;H^1(\mathbb{R}^N))^3\times L^2(0,T;H^1(\mathbb{R}^N))^3\times[a,b]^3\times L^2(\Omega)^3$.

To obtain the initial boundary condition of the steady state, we derive the Lagrangian $\mathcal{L}$ with respect to $\sigma = (\sigma_1, \sigma_2, \sigma_3)$, for all $\psi \in L^2(\Omega)$, it follows that

$$< \frac{\partial \mathcal{L}}{\partial \sigma_i}, \psi >= \int_\Omega \psi(c_i(0) - c_i^0)$$

for all $\psi \in L^2(\Omega)$ the last integral vanishes if and only if $c_i(0) = c_i^0$ in Ω.

To get the adjoint equation we derive the Lagrangian with respect to the state variable (c_1, c_2, c_3), for all $\varphi \in L^2(0, T; H^1(\mathbb{R}^N))$, one has

$$\begin{aligned}
< \frac{\partial \mathcal{L}}{\partial c_1}, \varphi >= & \int_0^T \int_\Omega \varphi(c_1 - c_1^{obs}) d\sigma dt + \int_0^T \int_\Omega \left(\frac{\partial \varphi}{\partial t} p_1 + D \nabla \varphi \nabla p_1 \right) \\
& + \int_0^T \int_\Omega \left(\nabla v \nabla p_1 + \lambda_1 p_1 - \lambda_1 p_2 \right) \varphi + \int_\Omega \sigma_1 \varphi(0), \\
< \frac{\partial \mathcal{L}}{\partial c_2}, \varphi >= & \int_0^T \int_\Omega \varphi(c_2 - c_2^{obs}) d\sigma dt + \int_0^T \int_\Omega \left(\frac{\partial \varphi}{\partial t} p_2 + D \nabla \varphi \nabla p_2 \right) \\
& + \int_0^T \int_\Omega \left(\nabla v \nabla p_2 + \lambda_2 p_2 - \lambda_2 p_3 \right) \varphi + \int_\Omega \sigma_2 \varphi(0), \\
< \frac{\partial \mathcal{L}}{\partial c_3}, \varphi >= & \int_0^T \int_\Omega \varphi(c_3 - c_3^{obs}) d\sigma dt + \int_0^T \int_\Omega \left(\frac{\partial \varphi}{\partial t} p_3 + D \nabla \varphi \nabla p_3 \right) \\
& + \int_0^T \int_\Omega \left(\nabla v \nabla p_3 + \lambda_3 p_3 \right) \varphi + \int_\Omega \sigma_3 \varphi(0).
\end{aligned}$$

We choose $\sigma_i(x, y) = p_i(x, y, 0)$, consequently the adjoint state is given as a solution $P = (p_1, p_2, p_3)$ of the following problem

$$\begin{cases}
-\frac{\partial p_1}{\partial t} = \nabla.(D.\nabla p_1) - \nabla p_1 \nabla v + \lambda_1 p_2 - \lambda_1 p_1 + c_1^{obs} - c_1 & \text{in} \quad \Omega \times]0, T[, \\
-\frac{\partial p_2}{\partial t} = \nabla.(D.\nabla p_2) - \nabla p_2 \nabla v + \lambda_2 p_3 - \lambda_2 p_2 + c_2^{obs} - c_2 & \text{in} \quad \Omega \times]0, T[, \\
-\frac{\partial p_3}{\partial t} = \nabla.(D.\nabla p_3) - \nabla p_3 \nabla v - \lambda_3 p_3 + c_3^{obs} - c_3 & \text{in} \quad \Omega \times]0, T[, \\
p_i(x, y, T) = 0 & \text{in} \quad \Omega, i \in \{1, 2, 3\}, \\
D \frac{\partial p_i}{\partial n} = 0 & \text{on} \quad \Gamma^0 \times]0, T[.
\end{cases} \tag{12}$$

To conclude the differentiability of J, we pass to derive the Lagrangian $\mathcal{L}$ with respect to $\Lambda = (\lambda_1, \lambda_2, \lambda_3)$, we have

$$\begin{aligned}
\frac{\partial \mathcal{L}}{\partial \lambda_1} &= \int_0^T \int_\Omega c_1(p_1 - p_2), \\
\frac{\partial \mathcal{L}}{\partial \lambda_2} &= \int_0^T \int_\Omega c_2(p_2 - p_3), \\
\frac{\partial \mathcal{L}}{\partial \lambda_3} &= \int_0^T \int_\Omega c_3 p_3.
\end{aligned}$$

Finally, we deduce the differentiability of J with respect to λ, moreover we have

$$\nabla J(\Lambda) = \left(\frac{\partial J(\Lambda)}{\partial \lambda_1}, \frac{\partial J(\Lambda)}{\partial \lambda_2}, \frac{\partial J(\Lambda)}{\partial \lambda_3} \right)$$

with (c_1, c_2, c_3) is solution of (4) and (p_1, p_2, p_3) is solution of the adjoint equation (12). □

5. PSOGSA algorithm

In this section we present the PSOGSA algorithm proposed by M. This algorithm is a hybridization of two meta heuristics. PSO proposed by Kennedy and Eberhart ([15][29]), and GSA proposed by E. Rashedi et al. [25].
We consider the following problem:

$$\min_{x\in\mathcal{D}} f(x) \tag{13}$$

where f is a function of $\mathbb{R}^p$ with value in $\mathbb{R}$ and $\mathcal{D}$ a bounded subset of $\mathbb{R}^p$.

5.1. PSO algorithm. Particle Swarm Optimization (PSO) is an evolutionary algorithm inspired from social behavior of bird flocking. The principle is to generate a number of particles (possible solutions) which fly around in the search space to find best solution.
At each iteration, each particle in the population represents the current position in $\mathcal{D}$ with the current velocity, it changes its velocity and position by considering the distance to pbest (personnal best position) and the distance to gbest (global best) that can be modeled mathematically by:

$$v_i^{n+1} = wv_i^n + c_1 \times rand \times (pbest_i^n - x_i^n) + c_2 \times rand \times (gbest - x_i^n), \tag{14}$$

$$x_i^{n+1} = x_i^n + v_i^{n+1}, \tag{15}$$

with
(1) v_i^n the velocity of the particle i at the n^{th} the iteration,
(2) w the inertia weight,
(3) c_1 and c_2 are the acceleration coefficients,
(4) $rand$ a random number between 0 and 1,
(5) x_i^n the position of the particle i at the n^{th} iteration,
(6) $pbest_i^n$ the $pbest$ of agent i at n^{th} iteration.

5.2. GSA algorithm. GSA is a heuristic optimization method proposed by E. Rashedi et al. [25]. This algorithm is inspired from the Newton's theory according to which "each particle particle in the universe attracts every other particle with a force that is directly proportional to the product of their masses and inversely proportional to the square of the distance between them". All masses attract each other by the gravitational forces between them.
In GSA, each mass has four characteristics: its position (X_i), inertial mass (M_{ii}), active gravitational mass (M_{ai}), passive gravitational mass (M_{ip}). The position of the mass in the search space represents a solution of the problem and its gravitational and inertial masses are determined using a fitness function of the problem.

Suppose a system with N agents in $\mathcal{D}$. The position of each agent is defined by:

$$X_i = (x_i^1, \cdots, x_i^d, \cdots, x_i^p), i = 1, 2, \cdots, N. \tag{16}$$

According to Newton gravitation theory, the gravitational forces from agent j on agent i at the time t is defined as follow

$$F_{ij}^d = G(t)\frac{M_{pi(t)\times M_{aj}(t)}}{R_{ij}(t)+\varepsilon}\big(x_j^d(t) - x_i^d(t)\big), \tag{17}$$

where $G(t)$ is gravitational constant at time t, ε is a small constant, and $R_{ij}(t)$ is the Euclidian distance between two agents i and j. $G(t)$ is given by

$$G(t) = G_0 \times exp(-\alpha \times \frac{iter}{Max_{iter}}), \tag{18}$$

where α and G_0 are descending coefficient and initial value respectively, $iter$ is the current iteration, and Max_{iter} is maximum number of iterations.

The total force acting on agent i is calculated by the following formula

$$F_i^d(t) = \sum_{j=1, j\neq i}^{N} a_j \times F_{ij}^d(t), \tag{19}$$

where a_j is a random number in the interval [0,1].
The accelaration γ_i^d of agent i is given by

$$\gamma_i^d(t) = \frac{F_i^d(t)}{M_{ii}(t)}. \tag{20}$$

Next velocity and position of agent i are calculated as follow:

$$v_i^d(t+1) = r_i \times v_i^d(t) + \gamma_i^d(t), \tag{21}$$

$$x_i^d(t+1) = x_i^d(t) + v_i^d(t+1), \tag{22}$$

where r_i is a random number in the interval [0,1].

5.3. PSOGSA algorithm. PSOGSA proposed by Mirjalili et al (2017) [24] combine the ability of social thinking ($gbest$) in PSO with the local search capability of GSA. The velocity of agent i is given by

$$V_i(t+1) = w \times V_i(t) + c_1' \times r_1 \gamma_i(t) + c_2' \times r_2 \times (gbest - X_i(t)), \tag{23}$$

where V_i is the velocity of agent i at iteration t, c_1' and c_2' are weighting factors, w is a weighting function, r_1 and r_2 are random numbers between 0 and 1, $\gamma_i(t)$ is the acceleration of agent i at iteration t.
The position X_i $(i = 1, \cdots, N)$, is given by

$$X_i(t+1) = X_i(t) + V_i(t+1). \tag{24}$$

5.4. Algorithm. In summary the resolution of our problem by PSOGSA algorithm is given the algorithm below:

6. Results and discussions

The parameters of flow simulation are:

D_m	α_T	α_L	S	K	ω
10^{-7}	0.01	0.1	0.02	0.001	0.33

TABLE 1. Parameters of flow.

Initialize the input parameters for PSO and GSA
Initialize the random position of search agents.
$k \leftarrow 0$
while $k < Max_iter$ **do**
  for i=1 to N **do**
    Solving equation (1)
    Solving equation (4)
    Evaluate the score of each search agent using objective function (11)
    Update the G and gBest for each agent
    Calculate M, forces and accelerations for all agents
    Update velocity and position for each agent
  end for
  $k \leftarrow k + 1$
end while
Return the best solution

6.1. Parameters identified. Using our algorithm on the data above, we obtain the following results:

Parameters	Range	Identified values
λ_1	$[0; 2]$	0.06242
λ_2	$[0; 2]$	0.789
λ_3	$[0; 3]$	1.08

The Figure 3 shows a comparison between the level simulated and observed data. In analyzing this figure, we see that the concentration simulated coincide with the concentration observed.

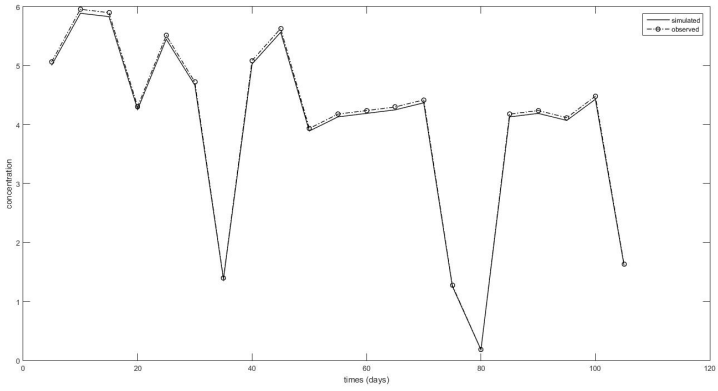

FIGURE 3. Curve of observed and simulated level to measurement dates.

6.2. Spatial distribution of NH_4^- concentration. The Figure 4 shows the removal rate of Nitrogen in the system. This rate increases at the beginning of the process to stabilize around 40% from the 30th day.

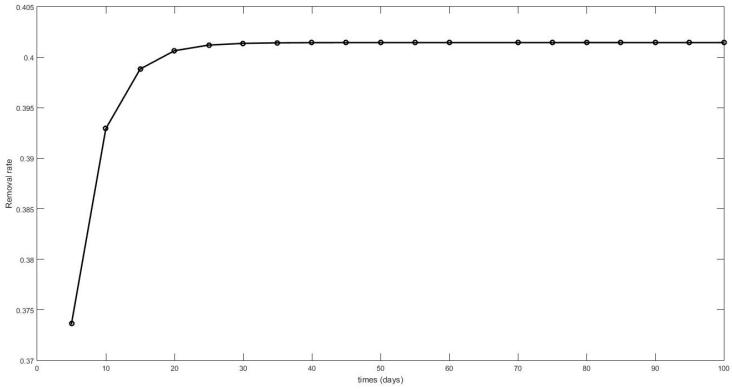

FIGURE 4. Curve of removal rate.

Figures 5 to 7 show spatial distribution of nitrogen in the system at different days respectively at 10, 50 and 100 days. As the case of the study on phosphorus in the [23], we note that concentrations vary considerably at the right and left borders of the system. They remain almost constant within the system.

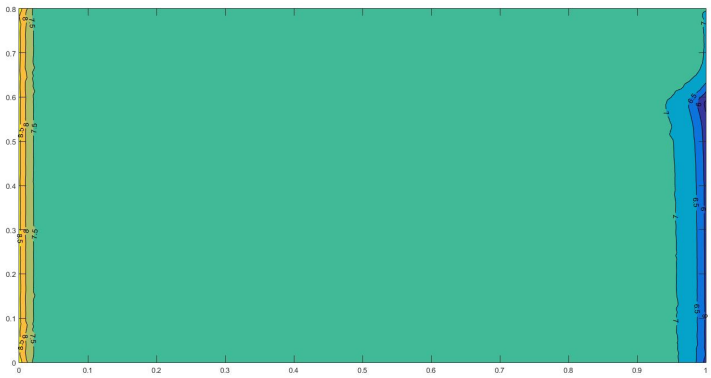

FIGURE 5. Day 10.

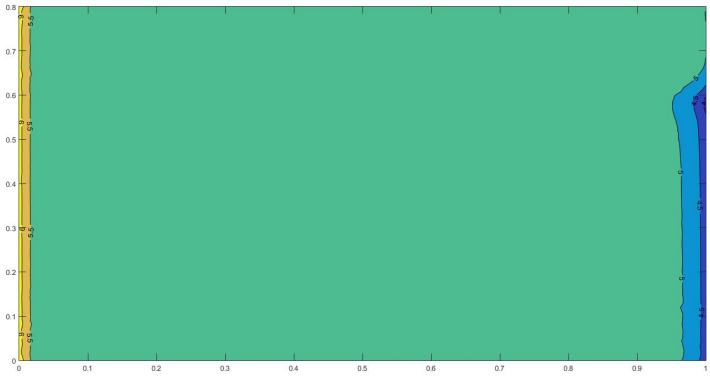

FIGURE 6. Day 50.

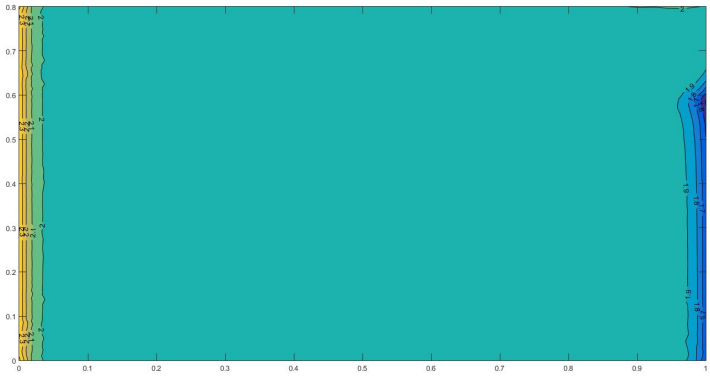

FIGURE 7. Day 100.

7. Conclusion

In this work, mathematical modeling and numerical simulation of hydrodynamics and nitrogen transformation processes in HSF constructed wetlands and porous media have been studied. The nitrogen kinetics has been modeled by hierarchical system of three advection dispersion-reaction equation. This system is solved by using the technique of operators splitting. The equation of advection is approximed by the Characteristics-Galerkin Method. The dispersion-reaction equation was carried by using the finite element method. The data used were measured in a bioreactor built in a primary school in Marrakech. Decay coefficient values, useful for design purposes, were determined by using Particle Swarm Optimization and Gravitational Search Algorithm (PSOGSA). The results of simulation show that the concentration of nitrogen simulated agrees fully with the one obtained by experimental data. The

removal rate of nitrogen in the system range between 37.5% and 40%.

References

[1] C.S. Akratos, V.A. Tsihrintzis, Effect of temperature, HRT, vegetation and porous media on removal efficiency of pilot-scale horizontal subsurface flow constructed wetlands, *Ecol. Eng.* **29** (2007), no. 2, 173–191.

[2] Association Francaise de Normalisation (AFNOR), *Recueil de Norme Francaise: Eau, Méthodes D'éssai*, 2eme édition, 1997.

[3] American Public Health Association (APHA), *Standard Methods for Analysis of Waste and Wastewater*, 18th Edition, Washington DC, 1992.

[4] J.M.H. Andersen, Influence of pH on release of phosphorus from lake sediments, *Arch. Hydrobiol.* **76** (1975), 411–419.

[5] S.K. Bastviken, S.E.B. Weisner, G. Thiere, J.M. Svensson, P.M. Ehde, K.S. Tonderski, Effects of vegetation and hydraulic load on seasonal nitrate removal in treatment wetlands, *Ecol. Eng.* **35** (2009), no. 5, 946–952.

[6] B.C. Braskerud, Factors affecting phosphorus retention in small constructed wetlands treating agricultural non-point source pollution, *Ecological Engineering* **19** (2002), no. 1, 41–61.

[7] J.N. Carleton, J. Montas, An analysis of performance models for free water surface wetlands, *Water Research* **25** (2007), 16–22.

[8] P.G. Ciarlet, *Introduction à l'Analyse Numérique Matricielle et à l'Optimisation*, Masson, Paris, 1982.

[9] T.P. Clement, Y. Sun, B.S. Hooker, J.N. Peterser, Modeling Multispecies Reactive Transport in Ground Water, *Groundwater Monitoring and Remediation* **18** (1998), 79–92.

[10] S. Descombes, Convergence of a splitting method of high order for reactiondiffusion systems, *Math. Comp.* **70** (2001), no. 263, 1481–1501.

[11] J.C. Germon, C. Henault *Quantifier la d'énitrification et la production naturelle de N2O dans les sols : synthèse bibliographique*, Ministère de l'Environnement, INRA DIJON, France, 1994.

[12] I.C.R. Holford, W.H. Patrick Jr., Effects of reduction and pH changes on phosphate sorption and mobility in an acid soil, *Soil Sci. Soc. Am. Journal Abs.* **43** (1979), no. 2, 292–297.

[13] R.H. Kadlec, R.L. Knight, *Treatment wetlands*, CRC Press/Lewis Publishers, Boca Raton, 1996.

[14] K. Karlsen, H. Risebro, An operator splitting for convection-diffusion equations, *Numer. Math.* **77** (1997), no. 3, 365–382.

[15] J. Kennedy, R. Eberhart, Particle swarm optimization, *Proceedings of IEEE international conference on neural networks* **4** (1995), 1942–1948.

[16] A.K. Kivaisi, The potential for constructed wetlands for wastewater treatment and reuse in developing countries: a review, *Ecol. Eng.* **16** (2001), no. 4, 545–560.

[17] G. Langergraber, Simulation of the treatment performance of outdoor subsurface flow constructed wetlands in temperate climates, *Science of The Total Environmentl* **380** (2007), no. 7, 210–219.

[18] E. Ledoux, *Modèles mathématiques en hydrogéologie*, Centre d'Informatique Géologique école Nationale Supérieure des Mines de Paris, 2003.

[19] E. Llorens, J. Obradors, M.T. Alarcon-Herrera, Modelling the non-biogenic steps of arsenic retention in horizontal subsurface flow constructed wetlands, *Chemical Engineering Journal*, **223** (2013), 657–664.

[20] G. Maltais-Landry, R. Maranger , J. Brisson, Effect of artificial aeration and macrophyte species on nitrogen cycling and gas flux in constructed wetlands, *Ecol. Eng.* **35** (2009), 221–229.

[21] G. de Marsily, *Quantitative hydrogeology: Groundwater Hydrology for engineers*, Academic Press, New York, 1986.

[22] P. Molle, *Filtres plantés de roseaux : limites hydrauliques et rétention du phosphore*, Thèse de Doctorat, Université de Montpellier II, France, 2003.

[23] I. Mouaouia, W.O. Sawadogo, J. Laaffat, H. Khalfi, N. Alaa, Mathematical Modeling and numerical simulation of Phosphorus Reactive transport in an Horizontal Subsurface Flow Constructed Wetland treating Greywater, *J. Adv. Math. Stud.* **11** (2018), no. 2, 347–358.

[24] S. Mirjalili, S.Z.M. Hashim, A new hybrid PSOGSA algorithm for function optimization, *IEEE* **5** (2017), 374–377.
[25] E. Rashedi, S. Nezamabadi, S. Saryazdi, GSA: A Gravitational Search Algorithm, *Informations Sciences* **179** (2009), no. 13, 2232–2248.
[26] C.J. Richardson, B.C. Craft, *Effective phosphorus retention in wetlands-fact or fiction. Constructed Wetlands for Water Quality Improvement*, Press/Lewis Publishers, 2003.
[27] J. Rodier, *L'analyse de L'eau: Eaux Naturelles, Eaux Résiduaires, Eau de Mer*, Dunod, Paris, 2009.
[28] R. Samso Campa, *Numerical modelling of Constructed Wetlands for wastewater treatment*, PhD Thesis, Universita Politcnica de Catalunya, 2014.
[29] Y. Shi, R. Eberhart, A modified particle swarm optimiser, *IEEE International conference on Evolutionary Computation* **1998** (1998), 69–73.
[30] E.J.W. Visser, T.D. Colmer, C.W.P.M. Blom, L.A.C.J. Volesenek, Changes in growth, porosity and radial oxygen loss from adventitious roots of selected mono and dicotyledonous wetland species with contrasting types of aerenchyma, *Plant Cell Environ.* **23** (2000), 1237–1245.
[31] D. Whitney, A. Rossman, N. Hayden, Evaluating an existing subsurface flow constructed wetland in Akumal, Mexico, *Ecol. Eng.* **20** (2003), 105–111.
[32] X.F. Xu, H.Q. Tian, Z.J. Pan, Modeling ecosystem responses to prescribed fires in a phosphorus-enriched everglades wetland: phosphorus dynamics and community shift in response to hydrological and seasonal scenarios, *Ecological Modelling* **222** (2011), 3942–3956.

(I. Mouaouia, A. Charkaoui, N. Alaa) Faculty of Science and Technology of Marrakech, University of Cadi Ayyad, Morroco
E-mail address: ihsane.mouaouia@gmail.com, charkaoui.abderrahim92@gmail.com, n.alaa@uca.ac.ma

(W. O. Sawadogo) University of Ouahigouya, Burkina Faso
E-mail address: wenddabo81@gmail.com